

# Strain-Induced Room-Temperature Ferromagnetic Semiconductors with Large Anomalous Hall Conductivity in Two-Dimensional $\text{Cr}_2\text{Ge}_2\text{Se}_6$

Xue-Juan Dong,<sup>1</sup> Jing-Yang You,<sup>1</sup> Bo Gu,<sup>2,3,\*</sup> and Gang Su<sup>1,2,3,†</sup>

<sup>1</sup>*School of Physical Sciences, University of Chinese Academy of Sciences, 100049 Beijing, China*

<sup>2</sup>*Kavli Institute for Theoretical Sciences, and CAS Center for Excellence in Topological Quantum Computation, University of Chinese Academy of Sciences, 100190 Beijing, China*

<sup>3</sup>*Physical Science Laboratory, Huairou National Comprehensive Science Center, 101400 Beijing, China*



(Received 16 January 2019; revised manuscript received 22 May 2019; published 11 July 2019)

By density-functional-theory calculations, we predict a stable two-dimensional (2D) ferromagnetic semiconductor,  $\text{Cr}_2\text{Ge}_2\text{Se}_6$ , where the Curie temperature  $T_C$  can be dramatically increased beyond room temperature by applying a few-percent strain. In addition, the anomalous Hall conductivity in 2D  $\text{Cr}_2\text{Ge}_2\text{Se}_6$  and  $\text{Cr}_2\text{Ge}_2\text{Te}_6$  is predicted to be comparable to that in the ferromagnetic metals Fe and Ni, and is an order of magnitude larger than that in the diluted magnetic semiconductor Ga(Mn,As). Based on superexchange interactions, the increased  $T_C$  in 2D  $\text{Cr}_2\text{Ge}_2\text{Se}_6$  caused by strain can be understood by the decreased energy difference between 3d orbitals of Cr and 4p orbitals of Se. Our findings highlight the microscopic mechanism to obtain room-temperature ferromagnetic semiconductors by strain.

DOI: [10.1103/PhysRevApplied.12.014020](https://doi.org/10.1103/PhysRevApplied.12.014020)

## I. INTRODUCTION

Combining magnetism and a semiconductor enables the development of magnetic semiconductors, a promising way to realize spintronic applications based on use of both charge and spin degrees of freedom in electronic devices [1,2]. The highest Curie temperature  $T_C$  of the most-extensively-studied magnetic semiconductor, (Ga,Mn)As, is 200 K [3], still far below room temperature. Room-temperature ferromagnetic (FM) semiconductors are highly required for applications. Recent advances in magnetism in two-dimensional (2D) van der Waals materials have provided a new platform for the study of magnetic semiconductors [4]. Ising ferromagnetism with out-of-plane magnetization was observed experimentally in monolayer  $\text{CrI}_3$  with  $T_C = 45$  K [5]. The Heisenberg ferromagnetic state was obtained experimentally in 2D bilayer  $\text{Cr}_2\text{Ge}_2\text{Te}_6$  with  $T_C = 28$  K [6], and the corresponding bulk was experimentally shown to be a layered ferromagnet with spin along the  $c$  axis and  $T_C = 61$  K [7]. A large remanent magnetization with out-of-plane magnetic anisotropy was recently reported experimentally in a 6-nm film of  $\text{Cr}_2\text{Ge}_2\text{Te}_6$  on the topological insulator  $(\text{Bi,Sb})_2\text{Te}_3$  with  $T_C = 80$  K [8]. The magnetic structure in monolayer  $\text{CrI}_3$  and  $\text{Cr}_2\text{Ge}_2\text{Te}_6$  was recently discussed in terms of Kitaev interaction [9]. Photoluminescence and magneto-optical effects have also been discussed [10,11].

Ferromagnetism with high  $T_C$  was also reported experimentally in monolayer  $\text{VSe}_2$  [12] and  $\text{MnSe}_2$  [13]. Despite the relatively small number of monolayer ferromagnetic materials realized experimentally, predicting promising candidates by first-principles calculations can provide a reliable reference for experiments [14,15]. Possible 2D ferromagnetic materials have also been studied by machine learning [16] and high-throughput calculations [17].

Several methods are used to control the magnetic states in these recently discovered 2D materials. By tuning of the gate voltage, switching between the antiferromagnetic (AFM) state and the ferromagnetic state in bilayer  $\text{CrI}_3$  was obtained experimentally [18]. With use of the gate voltage, enhancement of ferromagnetism in 2D  $\text{Fe}_3\text{GeTe}_2$  was recently observed experimentally [19]. In 2D transition-metal dichalcogenides, which are nonmagnetic, strain is used to modify the optical and electronic properties [20]. Strain was shown to affect ferromagnetism in monolayer  $\text{Cr}_2\text{Ge}_2\text{Te}_6$  [21] and  $\text{CrX}_3$  ( $X$  is Cl, Br, or I) [22]. The electric field effect was studied experimentally in magnetic multilayer  $\text{Cr}_2\text{Ge}_2\text{Te}_6$  [23]. Recently, heterostructures of these 2D materials have also been studied [24–26].

In this paper, by density-functional-theory (DFT) calculations we predict a stable 2D ferromagnetic semiconductor,  $\text{Cr}_2\text{Ge}_2\text{Se}_6$ . We find that  $T_C = 144$  K in  $\text{Cr}_2\text{Ge}_2\text{Se}_6$ , which can be increased to 326 K by application of 3% strain and to 421 K by application of 5% strain. On the other hand,  $T_C$  in the 2D semiconductor  $\text{Cr}_2\text{Ge}_2\text{Te}_6$  is about 30 K in our calculations, close to the value of 28 K recently obtained experimentally [6]. In addition,

\*gubo@ucas.ac.cn

†gsu@ucas.ac.cn

the anomalous Hall conductivity in 2D  $\text{Cr}_2\text{Ge}_2\text{Se}_6$  and  $\text{Cr}_2\text{Ge}_2\text{Te}_6$  is predicted to be comparable to that in the ferromagnetic metals Fe and Ni [27–29], and is an order of magnitude larger than that in the diluted magnetic semiconductor Ga(Mn,As) [30,31]. Strain is found to decrease the energy difference between  $3d$  orbitals of Cr and  $4p$  orbitals of Se, which induces enhanced ferromagnetic coupling based on the superexchange mechanism. Our findings highlight the microscopic mechanism to obtain room-temperature magnetic semiconductors by strain.

## II. CALCULATION METHODS

The DFT calculations are done with Vienna *ab initio* simulation package [32]. Spin-polarized calculations are performed with the projector-augmented-wave method, and generalized-gradient approximations in the Perdew-Burke-Ernzerhof exchange-correlation functional are used. Spin-orbit coupling is included in the calculations. Total energies are obtained with  $9 \times 9 \times 1$   $k$  grids by the Mohnkhorst-Pack approach. The lattice constants and atom coordinates are optimized with energy convergence of less than  $10^{-6}$  eV and force less than  $0.01$  eV/Å, where a large vacuum of  $20$  Å is used to model a 2D system. The phonon calculations are performed by density-functional perturbation theory with PHONOPY [33]. The size of the supercell is  $3 \times 3 \times 1$ , where the displacement is taken as  $0.01$  Å.

For the on-site Coulomb interaction  $U$  of the Cr ion, values in the range of  $3$ – $5$  eV are usually reasonable for  $3d$  transition-metal insulators [34], while a small value of  $U < 2$  eV was adopted in DFT calculations of 2D  $\text{Cr}_2\text{Ge}_2\text{Te}_6$  [6]. We fixed  $U$  at  $4$  eV in most of our following calculations for 2D  $\text{Cr}_2\text{Ge}_2\text{Te}_6$  and  $\text{Cr}_2\text{Ge}_2\text{Se}_6$ , and we discuss the effect of different  $U$  values later.

On the basis of the DFT results, the Curie temperature is calculated by Monte Carlo simulations [21,22] based on the 2D Ising model, where a  $60 \times 60$  supercell is adopted, and  $10^5$  steps are performed for every temperature to achieve equilibrium. The anomalous Hall conductivity is calculated with WANNIER90 [35] and WannierTools [36].

## III. CRYSTAL STABILITY

We study the stability of the 2D material  $\text{Cr}_2\text{Ge}_2\text{Se}_6$ . We propose this material guided by the 2D material  $\text{Cr}_2\text{Ge}_2\text{Te}_6$  recently reported experimentally, and we replace Te by Se. The crystal structure of  $\text{Cr}_2\text{Ge}_2\text{Se}_6$  is shown in Figs. 1(a) and 1(b), where the space-group number is  $162$  ( $P\bar{3}1m$ ). The structure is obtained by fully relaxed calculations. The optimized lattice constant of 2D  $\text{Cr}_2\text{Ge}_2\text{Se}_6$  is calculated as  $6.413$  Å, which is smaller than the lattice constant of  $\text{Cr}_2\text{Ge}_2\text{Te}_6$  obtained experimentally ( $6.8275$  Å). This is reasonable because Se has a smaller radius than Te. We examine the stability in terms of the phonon spectrum, where the Brillouin zone is shown in Fig. 1(c). As shown

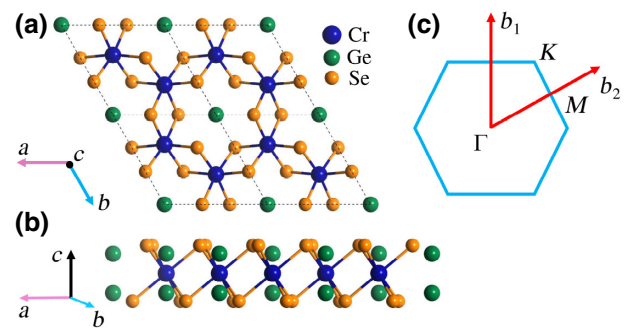


FIG. 1. Crystal structure of  $\text{Cr}_2\text{Ge}_2\text{Se}_6$ : (a) top view in the  $a$ - $b$  plane and (b) side view in the  $a$ - $c$  plane. The two-dimensional Brillouin zone is shown in (c).

in Fig. 2(a), there is no imaginary frequency in the phonon dispersion near the  $\Gamma$  point. This predicts that the crystal structure of monolayer  $\text{Cr}_2\text{Ge}_2\text{Se}_6$  is stable.

To further check the crystal stability, we study the formation energy of monolayer  $\text{Cr}_2\text{Ge}_2\text{Se}_6$  and  $\text{Cr}_2\text{Ge}_2\text{Te}_6$  by DFT calculations. The formation energy of  $\text{Cr}_2\text{Ge}_2\text{Se}_6$  is given by  $E_{\text{form}} = E_{\text{tot}} - 2E_{\text{Cr}} - 2E_{\text{Ge}} - 6E_{\text{Se}}$ , where  $E_{\text{tot}}$  is the total energy of 2D  $\text{Cr}_2\text{Ge}_2\text{Se}_6$ , and  $E_{\text{Cr}}$ ,  $E_{\text{Ge}}$ , and  $E_{\text{Se}}$  are the total energies per atom for the bulk chromium, germanium, and selenium, respectively. We find that the formation energy of monolayer  $\text{Cr}_2\text{Ge}_2\text{Se}_6$  is  $-1.13$  eV,

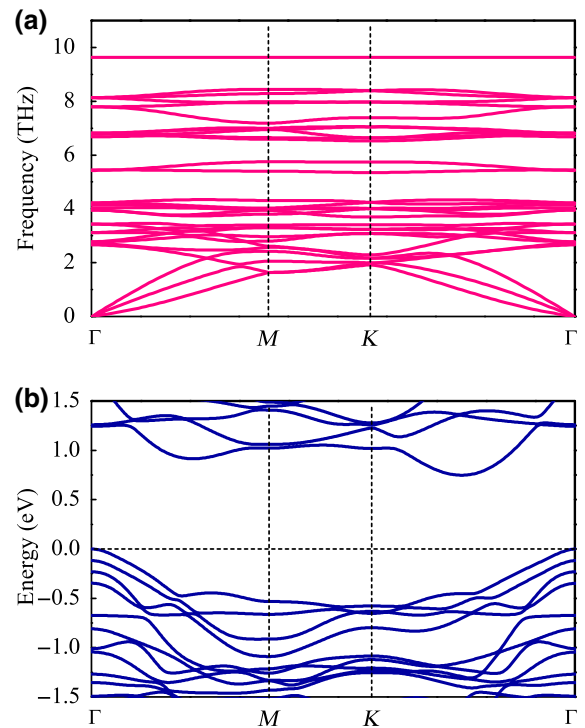


FIG. 2. (a) Phonon spectrum and (b) electronic band structure of two-dimensional  $\text{Cr}_2\text{Ge}_2\text{Se}_6$  obtained by spin-polarized generalized-gradient approximation plus spin-orbit coupling plus  $U$  calculations.

lower than the 0.92 eV of monolayer  $\text{Cr}_2\text{Ge}_2\text{Te}_6$ . This suggests that 2D  $\text{Cr}_2\text{Ge}_2\text{Se}_6$  should be stabler than 2D  $\text{Cr}_2\text{Ge}_2\text{Te}_6$  (the latter was recently realized experimentally [6]).

The electronic band structure of  $\text{Cr}_2\text{Ge}_2\text{Se}_6$  is shown in Fig. 2(b). An indirect band gap of 0.748 eV is observed, and monolayer  $\text{Cr}_2\text{Ge}_2\text{Se}_6$  is a semiconductor. Recently, it was found that the change of the magnetization direction can alter the band structure in 2D  $\text{CrI}_3$  [37]. In our case, we calculate the band structure of  $\text{Cr}_2\text{Ge}_2\text{Se}_6$  with in-plane magnetization, and find that the band structure does not change dramatically. In addition, we find that a larger band gap of 1.38 eV is obtained with use of the HSE06 hybrid functional, whereas the profiles of the band structure do not change.

#### IV. MAGNETIC PROPERTIES

To study the magnetic ground state of 2D  $\text{Cr}_2\text{Ge}_2\text{Se}_6$ , we examine the possible states with paramagnetic, ferromagnetic, and antiferromagnetic configurations. The calculations reveal that the energy of the paramagnetic state is 6 eV higher than the energy of the ferromagnetic and antiferromagnetic states. Figure 3(a) shows four possible magnetic states of 2D  $\text{Cr}_2\text{Ge}_2\text{Se}_6$ : the FM state, the AFM Néel state, the AFM stripe state, and the AFM zigzag state. The calculations show that the FM state is the stablest state, and the energy difference between the FM configuration and the AFM configuration is more than 30 meV (Table I). Furthermore, as shown in Fig. 3(b), the calculations show that the lowest energy of the ferromagnetic state is obtained when the magnetization direction is perpendicular to the two-dimensional materials, with magnetic anisotropy energy of 0.32 meV per unit cell of  $\text{Cr}_2\text{Ge}_2\text{Se}_6$ . The calculations show that for 2D  $\text{Cr}_2\text{Ge}_2\text{Se}_6$ , the spin momentum of a Cr atom is  $3.4\mu_B$  and the occupation number of Cr 3d orbitals is 3.976 (Table I).

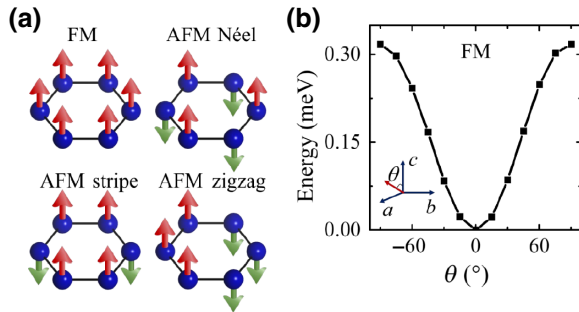


FIG. 3. (a) Four possible states for two-dimensional  $\text{Cr}_2\text{Ge}_2\text{Se}_6$ : FM state, AFM Néel state, AFM stripe state, and AFM zigzag state. Balls denote Cr atoms and arrows denote spins. (b) Total energy as a function of angle  $\theta$  for the FM state, obtained by spin-polarized generalized-gradient approximation plus spin-orbit coupling plus  $U$  calculations.

TABLE I. DFT results for the total energy of the ferromagnetic state  $E^{\text{FM}}$ , the total energy of the antiferromagnetic state  $E^{\text{AFM}}$ , the Curie temperature  $T_C$ , the 3d-orbital occupation number  $n_d$ , the spin ( $S$ ) and orbital ( $L$ ) momentum of the Cr atom, and the bond length  $d_{\text{Cr-Te(Se)}}$  for the 2D semiconductors  $\text{Cr}_2\text{Ge}_2\text{Te}_6$  and  $\text{Cr}_2\text{Ge}_2\text{Se}_6$ .

	$\text{Cr}_2\text{Ge}_2\text{Te}_6$	$\text{Cr}_2\text{Ge}_2\text{Se}_6$	
		No strain	5% strain
$E^{\text{FM}}$ (eV)	-89.1376	-97.3460	-96.5658
$E^{\text{AFM}}$ (eV)	-89.1309	-97.3135	-96.4710
$E^{\text{AFM}} - E^{\text{FM}}$ (meV)	6.7	32.5	98.8
$T_C$ (K)	30	144	421
$n_d$ (Cr)	4.043	3.976	3.951
$S$ ( $\mu_B$ ) (Cr)	3.586	3.404	3.487
$L$ ( $\mu_B$ ) (Cr)	-0.018	-0.076	-0.105
$d_{\text{Cr-Te(Se)}}$ (Å)	2.827	2.64	2.697

The Curie temperature  $T_C$  can be estimated by Monte Carlo simulations based on a 2D Ising model. The exchange-coupling parameter is estimated as the total energy difference between the ferromagnetic state and the antiferromagnetic state  $E^{\text{AFM}} - E^{\text{FM}}$  as listed in Table I, which was obtained by DFT calculations. The normalized magnetization obtained is shown as a function of temperature in Fig. 4(a). The experimental magnetization for  $\text{Cr}_2\text{Ge}_2\text{Te}_6$  is taken from the temperature-dependent Kerr rotation of bilayer  $\text{Cr}_2\text{Ge}_2\text{Te}_6$  with  $T_C = 28$  K [6]. The calculated Curie temperature is 30 K for monolayer  $\text{Cr}_2\text{Ge}_2\text{Te}_6$ , which is close to the experimental value. For simplicity the Ising model is applied in our Monte Carlo simulations, while the Heisenberg model with magnetic anisotropy was suggested from experiments [6]. In addition, the estimated Curie temperature  $T_C$  could be even larger if the mean-field approximation is used [17]. The calculated Curie temperature for monolayer  $\text{Cr}_2\text{Ge}_2\text{Se}_6$  is 144 K, which is about 5 times higher than the Curie temperature of 30 K for monolayer  $\text{Cr}_2\text{Ge}_2\text{Te}_6$  obtained by Monte Carlo simulations. More interestingly, the Curie temperature can be increased to 326 K by application of 3% tensile strain and to 421 K by application of 5% strain. We find that  $T_C$  is decreased to 67 K with 1% compression strain, as shown in Fig. 4(a), and the system becomes antiferromagnetic when 2% compression strain is applied. Our results predict that by application of a few-percent tensile strain monolayer  $\text{Cr}_2\text{Ge}_2\text{Se}_6$  could be a promising candidate for a room-temperature ferromagnetic semiconductor.

As the magnetization direction is out of the plane with an easy axis along the  $c$  direction in 2D  $\text{Cr}_2\text{Ge}_2\text{Te}_6$  and  $\text{Cr}_2\text{Ge}_2\text{Se}_6$ , it is interesting to study the anomalous Hall conductivity due to the Berry curvature of the band structure. The results obtained by DFT calculations are shown in Fig. 4(b). The magnitude of the anomalous Hall conductivity  $\sigma_{xy}$  for  $p$ -type  $\text{Cr}_2\text{Ge}_2\text{Se}_6$  and  $n$ -type  $\text{Cr}_2\text{Ge}_2\text{Te}_6$  can

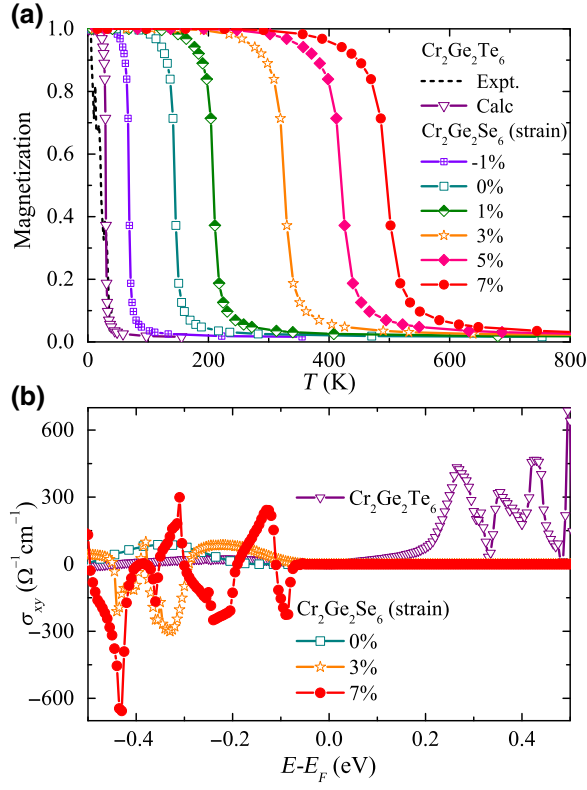


FIG. 4. (a) Normalized magnetization as a function temperature and (b) anomalous Hall conductivity as a function of energy for two-dimensional  $\text{Cr}_2\text{Ge}_2\text{Te}_6$  and  $\text{Cr}_2\text{Ge}_2\text{Se}_6$  with different strains. The experimental results for  $\text{Cr}_2\text{Ge}_2\text{Te}_6$  are taken from Ref. [6]. The calculated results are obtained by DFT calculations and Monte Carlo simulations.

be as large as  $4 \times 10^2$  ( $\Omega\text{cm}^{-1}$ ). This value is comparable to the value in some ferromagnetic metals, such as  $\sigma_{xy} = 7.5 \times 10^2$  in bcc Fe [27,28] and  $\sigma_{xy} = 4.8 \times 10^2$  ( $\Omega\text{cm}^{-1}$ ) in fcc Ni [29] due to the Berry curvature of the band structures. More importantly, the estimated  $\sigma_{xy}$  in the 2D magnetic semiconductors  $\text{Cr}_2\text{Ge}_2\text{Te}_6$  and  $\text{Cr}_2\text{Ge}_2\text{Se}_6$  is an order of magnitude larger than  $\sigma_{xy}$  of the classic diluted magnetic semiconductor Ga(Mn,As) [30,31].

TABLE II. DFT results for hopping-matrix element  $|V|$  and energy difference  $|E_p - E_d|$  between  $4p$  orbitals of Se and  $3d$  orbitals of Cr for the 2D semiconductor  $\text{Cr}_2\text{Ge}_2\text{Se}_6$  without strain and with 5% strain.

Strain (%)	Hopping-matrix element $ V $ (eV)				
	$p_z - d_{z^2}$	$p_z - d_{xz}$	$p_z - d_{yz}$	$p_z - d_{x^2-y^2}$	$p_z - d_{xy}$
0	0.257983	0.29527	0.380283	0.190041	0.445906
5	0.258289	0.22747	0.306872	0.201524	0.416315
Strain (%)	Energy difference $ E_p - E_d $ (eV)				
	$p_z - d_{z^2}$	$p_z - d_{xz}$	$p_z - d_{yz}$	$p_z - d_{x^2-y^2}$	$p_z - d_{xy}$
0	1.415092	0.4458	0.45512	0.581666	0.581166
5	1.552237	0.09143	0.09775	0.695055	0.693946

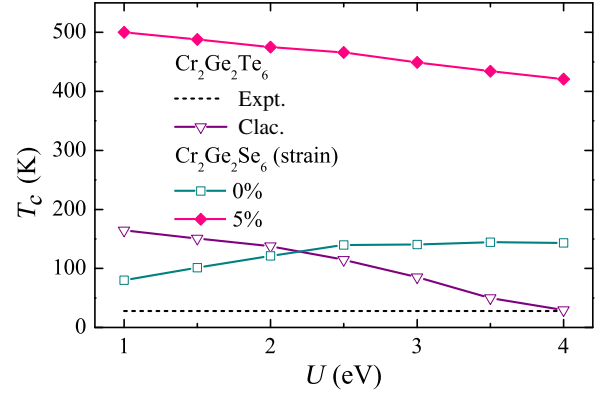


FIG. 5. Curie temperature  $T_C$  as a function of  $U$  for 2D  $\text{Cr}_2\text{Ge}_2\text{Te}_6$ ,  $\text{Cr}_2\text{Ge}_2\text{Se}_6$  without strain, and  $\text{Cr}_2\text{Ge}_2\text{Se}_6$  with 5% strain. The experimental results for  $\text{Cr}_2\text{Ge}_2\text{Te}_6$  and the calculated results are the same as in Fig. 4(a) but with different values of  $U$ .

## V. DISCUSSION

To study the effect of the on-site Coulomb interaction  $U$  of  $3d$  orbitals of Cr, we calculate the Curie temperature  $T_C$  as a function of  $U$  for 2D  $\text{Cr}_2\text{Ge}_2\text{Te}_6$ ,  $\text{Cr}_2\text{Ge}_2\text{Se}_6$  without strain, and  $\text{Cr}_2\text{Ge}_2\text{Se}_6$  with 5% strain, as shown in Fig. 5. The experimental  $T_C$  of 2D  $\text{Cr}_2\text{Ge}_2\text{Te}_6$  is taken from Ref. [6]. For 2D  $\text{Cr}_2\text{Ge}_2\text{Te}_6$ , the calculated  $T_C$  decreases with increasing  $U$ , and is close to the experimental  $T_C$  with  $U = 4$  eV. In addition, we find that the magnetization direction of  $\text{Cr}_2\text{Ge}_2\text{Te}_6$  becomes in plane with  $U = 1$  eV, which disagrees with the experimental results. The antiferromagnetic ground state is obtained for  $\text{Cr}_2\text{Ge}_2\text{Te}_6$  with  $U = 5$  eV, which also disagrees with the experimental results. Our calculations suggest that reasonable values of  $U$  for 2D  $\text{Cr}_2\text{Ge}_2\text{Te}_6$  may be in the range of 2–4 eV.

For 2D  $\text{Cr}_2\text{Ge}_2\text{Se}_6$  with 5% strain, the calculated  $T_C$  is always higher than room temperature with  $U$  in the range from 1 to 4 eV, as shown in Fig. 5. Thus, our prediction about the room-temperature ferromagnetic semiconductor  $\text{Cr}_2\text{Ge}_2\text{Se}_6$  with a few-percent strain is robust with the values of  $U$ .

How should we understand the increase of  $T_C$  in 2D  $\text{Cr}_2\text{Ge}_2\text{Se}_6$  caused by application of strain? Because of superexchange interaction [38–40], FM coupling is expected since the Cr—Se—Cr bond angle is close to  $90^\circ$ . The indirect FM coupling between Cr atoms is proportional to the direct AFM coupling between neighboring Cr and Se atoms. The magnitude of this direct AFM coupling can be roughly estimated as  $J = |V|^2/(|E_p - E_d|)$ , where  $|V|$  is the hopping-matrix element between  $4p$  orbitals of Se and  $3d$  orbitals of Cr and  $|E_p - E_d|$  is the energy difference between  $4p$  orbitals of Se and  $3d$  orbitals of Cr. By DFT calculations, we can obtain these parameters for 2D  $\text{Cr}_2\text{Ge}_2\text{Se}_6$  without strain and with 5% strain. The results for  $|V|$  and  $|E_p - E_d|$  are given in Table II. The results suggest that strain has little effect on the hopping-matrix element  $|V|$ , while strain can cause the energy difference between the  $p_z$  orbital of Se and the  $d_{xz}$  and  $d_{yz}$  orbitals of Cr to decrease to one fifth of the value without strain, causing a dramatic enhancement of the AFM coupling between Cr and Se atoms. This leads to enhanced FM coupling between Cr atoms, and results in  $T_C$  being above room temperature.

## VI. SUMMARY

By DFT calculations we predict a stable 2D ferromagnetic semiconductor,  $\text{Cr}_2\text{Ge}_2\text{Se}_6$ . We find the Curie temperature  $T_C$  of  $\text{Cr}_2\text{Ge}_2\text{Se}_6$  can be dramatically increased beyond room temperature by applying 3% strain, which is much higher than  $T_C = 28$  K in 2D  $\text{Cr}_2\text{Ge}_2\text{Te}_6$  recently observed experimentally. In addition, the anomalous Hall conductivity in 2D  $\text{Cr}_2\text{Ge}_2\text{Se}_6$  and  $\text{Cr}_2\text{Ge}_2\text{Te}_6$  is predicted to be an order of magnitude larger than that in the diluted magnetic semiconductor Ga(Mn,As). Based on superexchange interaction, the decreased energy difference between  $4p$  orbitals of Se and  $3d$  orbitals of Cr is found to be important to increase  $T_C$  in 2D  $\text{Cr}_2\text{Ge}_2\text{Se}_6$  caused by application of strain. Our findings highlight the microscopic mechanism to obtain room-temperature ferromagnetic semiconductors by strain.

## ACKNOWLEDGMENTS

The authors acknowledge Q.B. Yan, Z.G. Zhu, and Z.C. Wang for many valuable discussions. B.G. is supported by the National Natural Science Foundation of China (Grant No. Y81Z01A1A9), the Chinese Academy of Sciences (Grant No. Y929013EA2) and the University of Chinese Academy of Sciences (Grant No. 110200M208). G.S. is supported in part by the National Key R&D Program of China (Grant No. 2018FYA0305800), the Strategic Priority Research Program of the Chinese Academy of Sciences (Grants No. XDB28000000 and No. XBD07010100), the National Natural Science Foundation of China (Grant No. 11834014), and Beijing Municipal Science and Technology Commission (Grant No. Z118100004218001).

- [1] H. Ohno, Making nonmagnetic semiconductors ferromagnetic, *Science* **281**, 951 (1998).
- [2] T. Dietl, A ten-year perspective on dilute magnetic semiconductors and oxides, *Nat. Mater.* **9**, 965 (2010).
- [3] L. Chen, X. Yang, F. Yang, J. Zhao, J. Misuraca, P. Xiong, and S. von Molnár, Enhancing the curie temperature of ferromagnetic semiconductor (Ga,Mn)As to 200 K via nanostructure engineering, *Nano Lett.* **11**, 2584 (2011).
- [4] K. S. Burch, D. Mandrus, and J.-G. Park, Magnetism in two-dimensional van der Waals materials, *Nature* **563**, 47 (2018).
- [5] B. Huang, G. Clark, E. Navarro-Moratalla, D. R. Klein, R. Cheng, K. L. Seyler, D. Zhong, E. Schmidgall, M. A. McGuire, D. H. Cobden, W. Yao, D. Xiao, P. Jarillo-Herrero, and X. Xu, Layer-dependent ferromagnetism in a van der Waals crystal down to the monolayer limit, *Nature* **546**, 270 (2017).
- [6] C. Gong, L. Li, Z. Li, H. Ji, A. Stern, Y. Xia, T. Cao, W. Bao, C. Wang, Y. Wang, Z. Q. Qiu, R. J. Cava, S. G. Louie, J. Xia, and X. Zhang, Discovery of intrinsic ferromagnetism in two-dimensional van der Waals crystals, *Nature* **546**, 265 (2017).
- [7] V. Cartheaux, D. Brunet, G. Ouvrard, and G. Andre, Crystallographic, magnetic and electronic structures of a new layered ferromagnetic compound  $\text{Cr}_2\text{Ge}_2\text{Te}_6$ , *J. Phys.: Condens. Matter* **7**, 69 (1995).
- [8] M. Mogi, A. Tsukazaki, Y. Kaneko, R. Yoshimi, K. S. Takahashi, M. Kawasaki, and Y. Tokura, Ferromagnetic insulator  $\text{Cr}_2\text{Ge}_2\text{Te}_6$  thin films with perpendicular remanence, *APL Mater.* **6**, 091104 (2018).
- [9] C. Xu, J. Feng, H. Xiang, and L. Bellaiche, Interplay between kitaev interaction and single ion anisotropy in ferromagnetic  $\text{CrI}_3$  and  $\text{CrGeTe}_3$  monolayers, *npj Comput. Mater.* **4**, 57 (2018).
- [10] K. L. Seyler, D. Zhong, D. R. Klein, S. Gao, X. Zhang, B. Huang, E. Navarro-Moratalla, L. Yang, D. H. Cobden, M. A. McGuire, W. Yao, D. Xiao, P. Jarillo-Herrero, and X. Xu, Ligand-field helical luminescence in a 2D ferromagnetic insulator, *Nat. Phys.* **14**, 277 (2017).
- [11] Y. Fang, S. Wu, Z.-Z. Zhu, and G.-Y. Guo, Large magneto-optical effects and magnetic anisotropy energy in two-dimensional  $\text{Cr}_2\text{Ge}_2\text{Te}_6$ , *Phys. Rev. B* **98**, 125416 (2018).
- [12] M. Bonilla, S. Kolekar, Y. Ma, H. C. Diaz, V. Kalappattil, R. Das, T. Eggers, H. R. Gutierrez, M.-H. Phan, and M. Batzill, Strong room-temperature ferromagnetism in  $\text{VSe}_2$  monolayers on van der Waals substrates, *Nat. Nanotech.* **13**, 289 (2018).
- [13] D. J. O'Hara, T. Zhu, A. H. Trout, A. S. Ahmed, Y. K. Luo, C. H. Lee, M. R. Brenner, S. Rajan, J. A. Gupta, D. W. McComb, and R. K. Kawakami, Room temperature intrinsic ferromagnetism in epitaxial manganese selenide films in the monolayer limit, *Nano Lett.* **18**, 3125 (2018).
- [14] B. Shabir, M. Nadeem, Z. Dai, M. S. Fuhrer, Q.-K. Xue, X. Wang, and Q. Bao, Long range intrinsic ferromagnetism in two dimensional materials and dissipationless future technologies, *Appl. Phys. Rev.* **5**, 041105 (2018).
- [15] N. Sivadas, M. W. Daniels, R. H. Swendsen, S. Okamoto, and D. Xiao, Magnetic ground state of semiconducting

- transition-metal trichalcogenide monolayers, *Phys. Rev. B* **91**, 235425 (2015).
- [16] T. D. Rhone, W. Chen, S. Desai, A. Yacoby, and E. Kaxiras, Data-driven studies of magnetic two-dimensional materials, arXiv:1806.07989 (2018).
- [17] H. Liu, J.-T. Sun, M. Liu, and S. Meng, Screening magnetic two-dimensional atomic crystals with nontrivial electronic topology, *J. Phys. Chem. Lett.* **9**, 6709 (2018).
- [18] B. Huang, G. Clark, D. R. Klein, D. MacNeill, E. Navarro-Moratalla, K. L. Seyler, N. Wilson, M. A. McGuire, D. H. Cobden, D. Xiao, W. Yao, P. Jarillo-Herrero, and X. Xu, Electrical control of 2D magnetism in bilayer CrI<sub>3</sub>, *Nat. Nanotech.* **13**, 544 (2018).
- [19] Y. Deng, Y. Yu, Y. Song, J. Zhang, N. Z. Wang, Z. Sun, Y. Yi, Y. Z. Wu, S. Wu, J. Zhu, J. Wang, X. H. Chen, and Y. Zhang, Gate-tunable room-temperature ferromagnetism in two-dimensional Fe<sub>3</sub>GeTe<sub>2</sub>, *Nature* **563**, 94 (2018).
- [20] R. Roldán, A. Castellanos-Gomez, E. Cappelluti, and F. Guinea, Strain engineering in semiconducting two-dimensional crystals, *J. Phys.: Condens. Matter* **27**, 313201 (2015).
- [21] X. Li and J. Yang, CrXTe<sub>3</sub> (X = Si, Ge) nanosheets: Two dimensional intrinsic ferromagnetic semiconductors, *J. Mater. Chem. C* **2**, 7071 (2014).
- [22] J. Liu, Q. Sun, Y. Kawazoe, and P. Jena, Exfoliating bio-compatible ferromagnetic Cr-trihalide monolayers, *Phys. Chem. Chem. Phys.* **18**, 8777 (2016).
- [23] W. Xing, Y. Chen, P. M. Odenthal, X. Zhang, W. Yuan, T. Su, Q. Song, T. Wang, J. Zhong, S. Jia, X. C. Xie, Y. Li, and W. Han, Electric field effect in multilayer Cr<sub>2</sub>Ge<sub>2</sub>Te<sub>6</sub>: A ferromagnetic 2D material, *2D Mater.* **4**, 024009 (2017).
- [24] D. Zhong, K. L. Seyler, X. Linpeng, R. Cheng, N. Sivadas, B. Huang, E. Schmidgall, T. Taniguchi, K. Watanabe, M. A. McGuire, W. Yao, D. Xiao, K.-M. C. Fu, and X. Xu, Van der Waals engineering of ferromagnetic semiconductor heterostructures for spin and valleytronics, *Sci. Adv.* **3**, e1603113 (2017).
- [25] Z. Wang *et al.*, Electric-field control of magnetism in a few-layered van der Waals ferromagnetic semiconductor, *Nat. Nanotech.* **13**, 554 (2018).
- [26] M. Lohmann, T. Su, B. Niu, Y. Hou, M. Alghamdi, M. Aldosary, W. Xing, J. Zhong, S. Jia, W. Han, R. Wu, Y.-T. Cui, and J. Shi, Probing magnetism in insulating Cr<sub>2</sub>Ge<sub>2</sub>Te<sub>6</sub> by induced anomalous Hall effect in Pt, *Nano Lett.* **19**, 2397 (2019).
- [27] Y. Yao, L. Kleinman, A. H. MacDonald, J. Sinova, T. Jungwirth, D. Sheng Wang, E. Wang, and Q. Niu, First Principles Calculation of Anomalous Hall Conductivity in Ferromagnetic bcc Fe, *Phys. Rev. Lett.* **92**, 037204 (2004).
- [28] X. Wang, J. R. Yates, I. Souza, and D. Vanderbilt, Ab initio calculation of the anomalous Hall conductivity by Wannier interpolation, *Phys. Rev. B* **74**, 195118 (2006).
- [29] X. Wang, D. Vanderbilt, J. R. Yates, and I. Souza, Fermi-surface calculation of the anomalous Hall conductivity, *Phys. Rev. B* **76**, 195109 (2007).
- [30] T. Jungwirth, J. Sinova, K. Y. Wang, K. W. Edmonds, R. P. Campion, B. L. Gallagher, C. T. Foxon, Q. Niu, and A. H. MacDonald, Dc-transport properties of ferromagnetic (Ga,Mn)As semiconductors, *Appl. Phys. Lett.* **83**, 320 (2003).
- [31] J. Sinova, T. Jungwirth, S.-R. E. Yang, J. Kučera, and A. H. MacDonald, Infrared conductivity of metallic (III,Mn)V ferromagnets, *Phys. Rev. B* **66**, 041202 (2002).
- [32] G. Kresse and J. Furthmüller, Efficient iterative schemes for ab initio total-energy calculations using a plane-wave basis set, *Phys. Rev. B* **54**, 11169 (1996).
- [33] A. Togo and I. Tanaka, First principles phonon calculations in materials science, *Scr. Mater.* **108**, 1 (2015).
- [34] S. Maekawa, T. Tohyama, S. E. Barnes, S. Ishihara, W. Koshibae, and G. Khaliullin, *Physics of Transition Metal Oxides*, Series in Solid State Sciences Vol. 144 (Springer, Berlin Heidelberg, 2004).
- [35] A. A. Mostofi, J. R. Yates, G. Pizzi, Y.-S. Lee, I. Souza, D. Vanderbilt, and N. Marzari, An updated version of wannier90: A tool for obtaining maximally-localised Wannier functions, *Comput. Phys. Commun.* **185**, 2309 (2014).
- [36] Q. Wu, S. Zhang, H.-F. Song, M. Troyer, and A. A. Soluyanov, WannierTools: An open-source software package for novel topological materials, *Comput. Phys. Commun.* **224**, 405 (2018).
- [37] P. Jiang, L. Li, Z. Liao, Y. X. Zhao, and Z. Zhong, Spin direction-controlled electronic band structure in two-dimensional ferromagnetic CrI<sub>3</sub>, *Nano Lett.* **18**, 3844 (2018).
- [38] J. B. Goodenough, Theory of the role of covalence in the perovskite-type manganites [LaM(II)]MnO<sub>3</sub>, *Phys. Rev.* **100**, 564 (1955).
- [39] J. Kanamori, Crystal distortion in magnetic compounds, *J. Appl. Phys.* **31**, S14 (1960).
- [40] P. W. Anderson, New approach to the theory of superexchange interactions, *Phys. Rev.* **115**, 2 (1959).